

PET/Cloisite[®]15A composite fibers – studies on the structure and the flame inhibition mechanism^{*})

Janusz Fabia^{1), **)}, Andrzej Gawłowski¹⁾, Monika Rom¹⁾, Czesław Ślusarczyk¹⁾, Włodzimierz Biniś¹⁾, Anna Brzozowska-Stanuch²⁾, Michał Puchalski³⁾

DOI: dx.doi.org/10.14314/polimery.2020.9.4

Abstract: The improvement of poly(ethylene terephthalate) (PET) fibers flame retardancy is usually achieved by using antipyrenes, which may be incorporated into polyester molecules during polycondensation or are physically mixed with polymer in the fiber formation process. In this article we present an alternative method to reduce the flammability of PET fibers and fabrics which is analogous to dyeing them with a dispersed dyes in a high temperature bath. We have tested this method many times using various modifiers so far. This time, we applied a commercial organophilized montmorillonite Cloisite[®]15A (C15A). In the presented work, using Limited Oxygen Index (LOI) flammability tests and the thermogravimetric analysis (TGA) method, the effectiveness of the modification used was demonstrated and its optimal variant was determined. Based on Fourier Transform-Infrared Spectroscopy (FT-IR) studies, the existence of interactions between PET macromolecules and the C15A modifier in the entire temperature range of the oxidative degradation was confirmed. Using the Wide-Angle X-ray Scattering (WAXS) and Small-Angle X-ray Scattering (SAXS) methods, the basic parameters of the nanostructure of the studied fibers were determined, and their nanocomposite nature was confirmed. The most important goal, which was successfully achieved, was to explain the mechanism of flame inhibition by the applied modifier C15A.

Keywords: PET fibers, Cloisite[®]15A, flame retardancy, LOI, TGA, FT-IR, SEM, WAXS, SAXS.

Włókna kompozytowe PET/Cloisite[®]15A – badania struktury i mechanizmu inhibitowania płomienia

Streszczenie: Poprawę właściwości palnych włókien poli(tereftalanu etylenu) (PET) można uzyskać w wyniku zastosowania uniepalniaczy, które mogą być wprowadzane do mieszaniny reakcyjnej podczas polikondensacji poliestru lub fizycznie mieszane z polimerem w procesie tworzenia włókien. W niniejszym artykule przedstawiono alternatywną metodę zmniejszania palności włókien i wyrobów tekstylnych z PET, analogiczną do procesu ich barwienia rozproszonymi barwnikami w kąpeli wysokotemperaturowej. Metodę tę testowaliśmy już wielokrotnie przy użyciu różnych modyfikatorów. Tym razem zastosowaliśmy handlowo dostępny organofilizowany montmorylonit Cloisite[®]15A (C15A). Za pomocą testów palności (określano wartość *LOI* – wskaźnika tlenowego) oraz analizy termogravimetrycznej (TGA) wykazano skuteczność zastosowanej modyfikacji i określono jej optymalny wariant. Na podstawie badań spektroskopowych FT-IR (spektroskopia w podczerwieni z transformacją Fouriera) potwierdzono występowanie oddziaływań między makrocząsteczkami PET i modyfikatora C15A w całym zakresie temperatury, obejmującym proces degradacji oksydacyjnej. Metodami szeroko i mało kątowej dyfrakcji rentgenowskiej (WAXS i SAXS) określono podstawowe parametry nanostruktury badanych włókien oraz potwierdzono ich nanokompozytowy charakter. Wyjaśniono także mechanizm inhibitowania płomienia przez zastosowany modyfikator C15A.

Słowa kluczowe: włókna PET, Cloisite[®]15A, zmniejszona zapalność, LOI, TGA, FT-IR, SEM, WAXS, SAXS.

¹⁾ University of Bielsko-Biala, Institute of Textile Engineering and Polymer Materials, Willowa 2, 43-309 Bielsko-Biała, Poland.

²⁾ BOSMAL Automotive Research and Development Institute Ltd, Sarni Stok 93, 43-300 Bielsko-Biała, Poland.

³⁾ Lodz University of Technology, Faculty of Material Technologies and Textile Design, Żeromskiego 116, 90-924 Łódź, Poland.

^{*}) Material contained in this article was presented at the XI International Conference on "X-ray Investigations of Polymer Structure", 3–6 December 2019, Ustroń, Poland.

^{**)} Author for correspondence: jfabia@ath.bielsko.pl

In recent years, the importance of nanoclay used to modify polymers increased, thus resulting in an improvement in polymer performance characteristics (including fire resistance). Nanoclays used as an additive to the polymer melt significantly improve the flame retardant properties of the material, especially if they are used in synergistic systems with other non-halogen flame retardants [1–6].

The development of polymer/layered silicate nanocomposites (PLSN) systems has enjoyed great interest in the last decade as a result of numerous improvements in the properties of these materials [7–9]. Montmorillonite (MMT) is the clay that is most commonly used to obtain PLSN. MMT is a silicate, the structure of which consists of several layers, with a layer thickness of about 0.96 nm and a transverse dimension of 100–200 nm [10]. The layers are piled with a regular gap, called the interlayer or gallery space, between them. The sum of the layer thickness and the interlayer space is a repeating unit of the lamellar stack of the material, called the long period, d -space or base space (d_{001}).

Standard PET fibers are not very resistant to fire and large amounts of smoke are emitted during their combustion. In addition, the so-called dripping effect (detached drops of molten polymer burn and promote the spread of fire) is characteristic of burning polymer. Therefore, giving PET fibers flame retardant properties and resistance to “dripping” is of particular interest to researchers [11]. The flame retarding modification of PET can be obtained in various ways. Most often, a properly ground (micro- or nano-) flame retardant substance is added to the polymer melt [12–14], but a surface application of the flame retardant is also used in the impregnation process [15–19]. A chemical method is used less often to obtain such characteristics [20].

An important technological parameter when adding clay nanoparticles to the polymer melt is their dispersion. Electron microscopy (TEM) and X-ray diffraction (XRD) methods are particularly useful for assessing dispersion in a polymer matrix. The interpretation of measurement results using these methods has been comprehensively described in the literature [21].

Structural changes are another equally important aspect of montmorillonite impact on the polymer matrix. In publications [22, 23], the authors examined the effect of nanoclay addition to the melt on the supermolecular structure of a PET matrix. The presence of MMT layered aluminosilicate particles in the PET matrix affects the crystallization of the polymer, reduces the glass transition temperature and leads to heterogeneous nucleation of the composite. As a result, the dyeing properties of PET were improved [22]. Studies have shown that the addition of clay causes a decrease in the crystallization temperature. This means that organophilized montmorillonite promotes the nucleation of PET crystallization and even a small amount of modified clay is sufficient to maximize the nucleation effect [23]. In addition, surface morphology studies using the TEM method showed partial peeling of the surface structure of the PET-CLAY nanocomposite film (with 3 wt % addition of C30B) [24].

Moreover, it should be noted that the production of fibers from thermoplastic polymers with the addition of nanoclay using extruder method is significantly hindered. An example would be the process of spinning and stretching polypropylene fibers with an addition of more than 1 wt % of clay, which is technically unacceptable due to the loss of the polymer melt spinning capacity [25].

An effective way of increasing fire resistance is also coating the finished materials with special pastes containing an addition of a flame retardant. However, the obtained coatings change the surface and performance properties of processed products [26, 27]. The authors of the publication [26] demonstrated that the use of nanoclay for paint coatings in optimal amounts of 3–5 wt % significantly improves the flame retardancy of the impregnated product. Addition of nanoclay below 1 wt % and above 10 wt % does not result in the desired effects.

In publication [28], the authors described the method of applying nanoclay in the form of an aqueous dispersion on cotton fabric. In this way, the *LOI* value increase by 4% in the case of nanoclay processing was obtained, while for fabric activated with low-temperature plasma in nitrogen and treated with nanoclay, a 5% increase in limited oxygen index was noted (this is the effect of synergistic interactions, as reported in the previously discussed publications).

However, there are no reports in the literature about the use of the same type of aqueous dispersion of organophilized aluminosilicate for the preparation of flame retardant polyester fibers. Therefore, in order to fill this gap, the water dispersion of commercial montmorillonite Cloisite 15A (in the form of nanoparticles) was used for the flame-retardant modification of PET fibers. The application process was carried out using the pressure method in a water bath (HT) as in the case of dyeing with suspension dyes. The mechanism of introducing C15A clay nanoparticles into the fiber material is based on the so-called “void” model [29]. This method has been used many times by us for flame retardant modification of PET fibers [30–32]. The obtained modified PET fibers were subjected to *LOI* flammability tests and detailed tests using such techniques as TGA, SEM, FT-IR, WAXS and SAXS. This article describes research aimed primarily at determining the mechanism of flame inhibition as a result of the use of aluminosilicate.

EXPERIMENTAL PART

Materials

The materials used in this work were all commercially available technical products.

PET fibers were supplied by Elana SA Toruń (Poland). As the flame retardant modifier – organophilic montmorillonite (MMT) in the form of nanoclay of type Cloisite®15A, produced by Southern Clay Product Inc. (USA), was used (Fig. 1) [33].

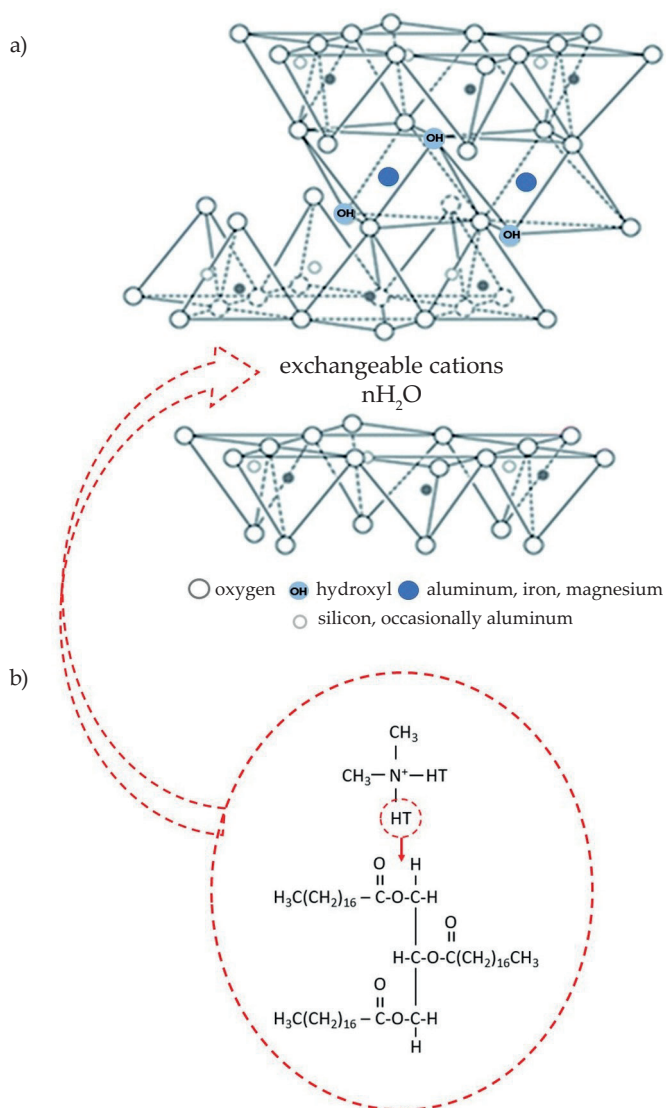


Fig. 1. Structure of: a) natural MMT, b) dimethyl, dehydrogenated tallow, quaternary ammonium organic modifier [33]

The clay was modified with quaternary ammonium salt. The finishing treatment of fibers was carried out in the laboratory dyeing device (Ahiba Turbomat, Switzerland) with a liquor ration of 1:50. The applied conditions were as following: temperature 130°C, treatment time 1 h and heating rate 2.5°C/min, respectively. The PET fibers were processed in an aqueous dispersion containing the C15A modifier and ROKAcet KO300G (Glyceryl Cocoate; CAS no. 68201-46-7) – nonionic surfactant (supplied by PCC Group, Poland) which was added into the bath in the amount of 0.7 g/dm³. C15A nanoclay dispersion was prepared using an ultrasonic bath for 15 min. After the modification treatment investigated samples were washed in a solution of detergent Pretepon G (PCC Group, Poland) in the amount of 5 g/dm³. The washing time was 30 min and the temperature 60°C. The effectiveness of the modifier was tested in a wide range of flame retardant concentrations from 0 to 7.5% in relation to the fiber weight.

Methods of testing

The examinations of the fiber flammability were carried out with the Limited Oxygen Index (LOI) method in accordance with PN ISO 4589.

Thermogravimetric Analysis (TGA) investigations were performed using Thermogravimetric Analyzer Q500 TA Instruments (USA). Measurements were done in a temperature range from 30 to 700°C with the heating rate of 10°C/min in air atmosphere (flow 40 cm³/min). Pre-tared platinum pans were used to contain the samples, and the samples were between 20 and 30 mg in size. The data were evaluated by means of the Universal V4.5A (TA Instruments) software.

Scanning Electron Microscopy (SEM) analyses were performed in conventional SEM mode using Joel JSM 5500LV instrument operating at 10 kV, after coating the samples with a thin layer of gold by sputter deposition. Surfaces of samples and scorching after the process of burning of PET fibers were observed with different magnifications.

Fourier Transform Infrared Spectroscopy (FT-IR) measurements were performed using a Nicolet 6700 FT-IR spectrometer (Thermo Electron Corp., Madison, USA) equipped with diffusion accessory EasiDiff (Thermo Nicolet Industries). The following measurement parameters were used: resolution 8 cm⁻¹; spectral range 500–4000 cm⁻¹; DTGS detector; number of scans – 64 of the solid samples. Data collection and post-processing were performed using OMNIC software (v. 8.0, Thermo Electron Corp.).

The Wide-Angle X-Ray Scattering (WAXS) investigations were carried out with a URD-65 Seifert (Germany) diffractometer. CuK α radiation was used at 40 kV and 30 mA. Monochromatization of the beam was obtained by means of a nickel filter and a graphite crystal monochromator placed in the diffracted beam path. A scintillation counter was used as a detector. Investigations were performed in the range of the angle 3° to 40° in steps of 0.1°.

The Small Angle X-Ray Scattering (SAXS) investigations were performed by means of a MBraun camera, which utilizes conventional Kratky collimation system. The front of the camera was directly mounted on the top of the tube shield of a stabilized Philips PW 1830 X-ray generator. The X-ray tube was operated at a power of 1.5 kW. CuK α radiation was used. Scattered radiation was recorded in acquisition time of 1200 s by means of a MBraun linear position-sensitive detector, model PSD 50. The detector had 1024 channels with a channel-to-channel distance of 52 μ m.

RESULTS AND DISCUSSION

As noted in the introduction, the main purpose of the research presented in this article was to determine the mechanism of flame inhibition in the case of PET fibers modified with organophilized C15A aluminosilicate. However, the presentation of the results begins with research on the effectiveness of the introduction of the flame retardant into the fiber material.

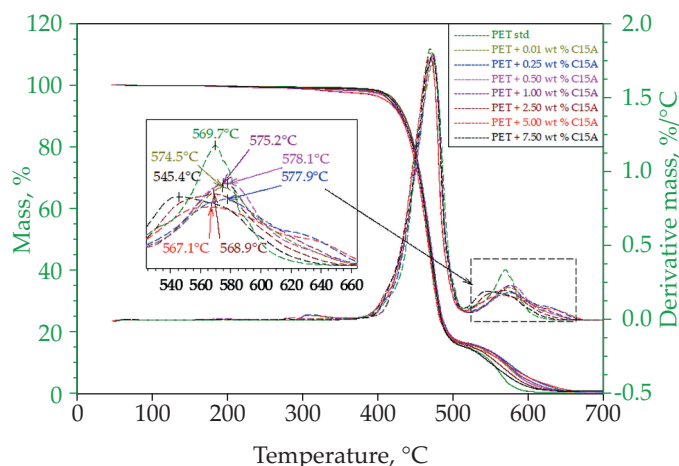


Fig. 2. TG and DTG curves of PET fibers modified with Cloisite®15A in the bath of 130°C; heating rate 20°/min, purge air flow 60 cm³/min

Effectiveness of the applied flame retardant application

The resulting flame retardant effect of PET fibers was evaluated using the limiting oxygen index method. A parameter that characterizes the method is the lowest percentage of oxygen in the mixture with nitrogen, at which the test specimen ignites and burns on its own. The effectiveness of the flame retardant action was tested in a wide range of C15A nanoclay content in the modifying bath: from 0 up to 7.5% in relation to the fiber weight.

Based on the analysis of *LOI* values obtained for individual modification variants, we found that the addition of C15A clay nanopowder actually affects the change in the limited oxygen index. These changes are not big, but they are undoubtedly significant. When relatively small amounts of the modifier of 0–0.5 wt % were used, a systematic, monotonic increase in the *LOI* value from 21.6% to 24.0% could be observed. Further increase in the modifier content resulted in a systematic reduction of the *LOI* value. The addition of nanoclay above 2.5 wt % caused the limited oxygen index to drop to even lower values than for combustion of PET fibers without a modifier.

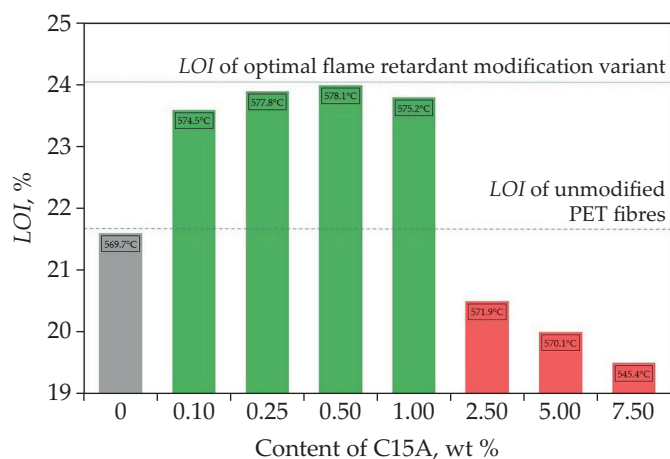
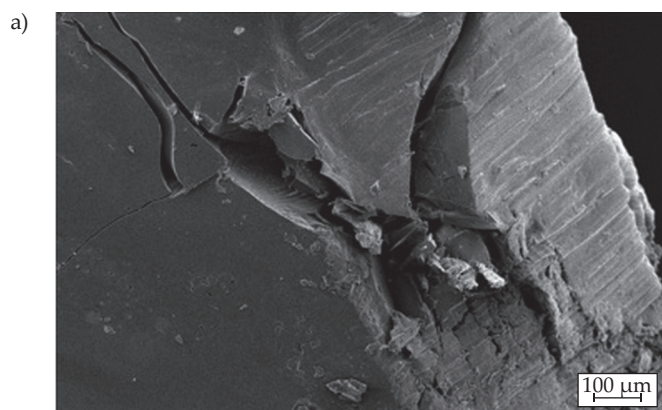


Fig. 3. The *LOI* values determined during the fibers burning tests depending on the variant of the flame retardant modification (*i.e.* amount of C15A modifier used): for each variant, the temperatures of the highest rate of mass loss during burning of the samples were marked

Confirmation of the improvement of the combustibility properties of the tested fibers, shown in *LOI* tests, was obtained by carrying out thermogravimetric tests in the air. For polymers such as PET, for which thermolysis in an oxidizing atmosphere and direct combustion of residues after this thermolysis are almost fully separable transformations, the application of the TGA method gives very good results. We have shown this before, both for classic PET fibers [30] and partially oriented PET fibers (POY) formed at high speeds [34]. Based on the analysis of the DTG curves it is possible to show the shift of the exothermic peak (and its maximum) corresponding to the sample combustion process. When the material is modified with flame retardant, the peak shifts towards higher temperatures.

In our case, the maximum of the discussed effect (Fig. 2) shifted from a temperature of 569.7°C for pure PET to a temperature of 578.1°C for the most favorable modification variant – 0.5 wt % of C15A.

With a further increase of the modifier content, up to 7.5 wt % of C15A, the opposite trend was observed, *i.e.* the shift of the discussed maximum towards lower tempera-

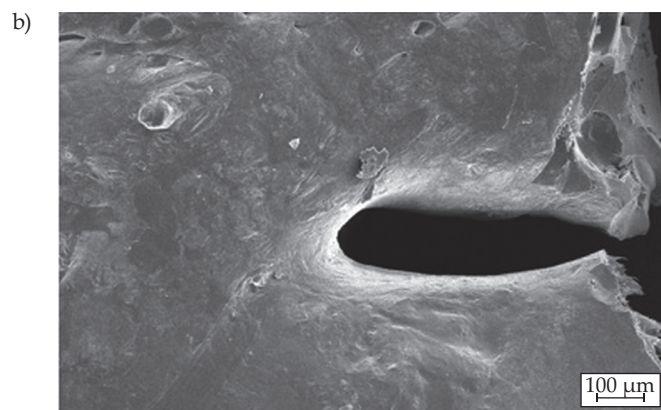


Fig. 4. SEM microphotographs of residue after combustion of: a) sample of unmodified PET fibers, b) PET fibers modified with C15A (0.5 wt %, 130°C)

tures. The obtained results clearly confirm the results of LOI tests and indicate a real improvement in the combustion properties of the tested PET fibers, but only within a specific range of nanoclay content, which is presented suggestively in Fig. 3.

For the optimum option of the flame-retardant modification of fibers (0.5 wt % of C15A addition) determined on the basis of LOI and TGA studies, tests of controlled combustion of the sample in atmospheric air were conducted, analysing both the combustion process itself and conducting microscopic observation of the scale formed after ignition of the sample. It turned out that during the combustion of nanoclay-modified fibers characteristic phenomenon of so-called “dropping” of molten, burning material, which occurs in the case of raw PET and can drastically contribute to the propagation of the flame zone during a fire, was not observed. SEM microscopic observations for scale samples (Fig. 4) resulting from the combustion of PET containing the C15A modifier (Fig. 4b) reveal a very clear difference with respect to the material without flame retardant modification (Fig. 4a).

The scale surface in the case of a sample with nanoclay is covered with a characteristic coating. Because the scale layer is formed in the immediate vicinity of the flame, the discussed coating effectively limits the access of flammable decomposing gases released during thermal dissociation of PET to the flame zone. Therefore, even after direct ignition of the material, we observe a tendency to retard and limit flame propagation. Additional information on the structure of the discussed coating was provided by the FT-IR spectroscopic tests and X-ray diffraction tests described later in the article.

FT-IR studies of fibers, C15A modifier and solid residue arising in the process of their oxidative degradation

Another important issue we decided to touch upon in the study of flame retardant modified polyester fibers with C15A nanoclay applied in water bath in a high-

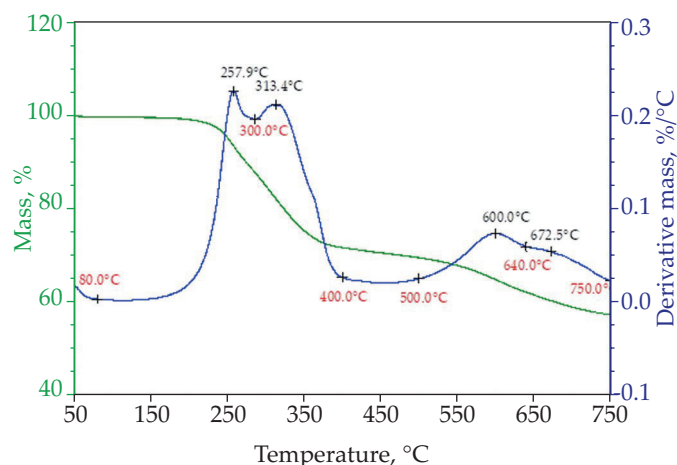


Fig. 5. TG and DTG curves of C15A clay with marked of FT-IR analysis temperature points (red)

temperature impregnation process was to determine the possible interactions between the fiber material – poly(ethylene terephthalate) and modifier particles. FT-IR spectroscopic tests were carried out in a wide temperature range of 0–750°C for samples previously heated in a TGA analyzer cell. The spectra were recorded and analyzed at characteristic temperatures determined on the basis of the DTG curves (Fig. 5).

These temperatures corresponded to the state of the samples after specific thermal changes, which actually took place during the oxidative degradation process of the modified fiber material.

Figure 6 summarizes the FT-IR spectra for C15A clay samples at room temperature and C15A modifier samples obtained at characteristic temperatures determined based on DTG curves.

The FT-IR spectrum recorded for C15A nanoclay at 25°C (Fig. 6) has a number of characteristic absorption bands. The band at 3630 cm^{-1} corresponds to the stretching vibrations of $[\text{N}-\text{H}]^+$ oscillators or at the same time vibrations of $-\text{OH}$ groups free from hydrogen bonding. Absorption bands at 2920 and 2850 cm^{-1} are stretching vibrations of $\text{C}-\text{H}$ oscillators. While the absorption band at 1468 cm^{-1} is deformation vibrations of $\text{C}-\text{H}$ oscillators. As a result of heating C15A clay to 400°C, the intensity of absorption bands decreases at 3630 cm^{-1} , and at 2920, 2850, 1468 cm^{-1} . After treatment at 500°C, we can observe the complete disappearance in the spectrum of absorption bands at 2920, 2850, 1468 cm^{-1} . After C15A heat treatment to 640°C in the FT-IR spectrum, we observe the appearance of absorption bands at 1625 cm^{-1} corresponding to oscillations of the $\text{C}=\text{C}$ oscillators, absorption bands at 1210 cm^{-1} corresponding to vibrations of the $-\text{C}-\text{O}-$ oscillators in carboxyl groups. After heating the nanoclay up to 750°C on the spectrum we observe a shift of this band to 1280 cm^{-1} .

Heating of the C15A clay causes thermal decomposition of the organic matter, which can be seen in spectra. Significant differences are observed in the spectra recorded for C15A nanoclay heated above 400°C with the disappearance of $\text{C}-\text{H}$ oscillator bands for maxima at

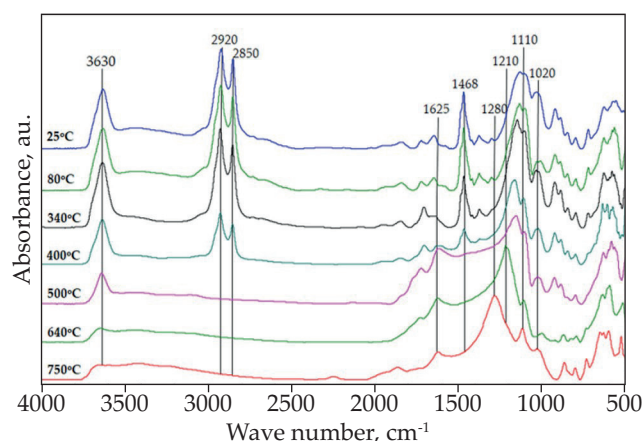


Fig. 6. FT-IR spectra of C15A clay after TGA test at different temperatures at air atmosphere

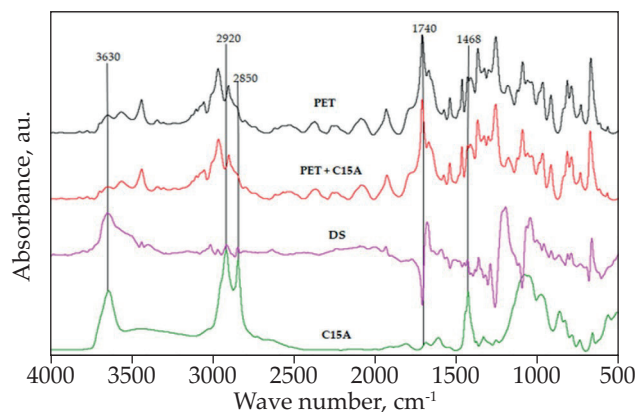


Fig. 7. FT-IR spectra of pure PET, PET + C15A, C15A clay and differential spectrum (DS) of PET + C15A and PET

2920 cm^{-1} ; 2850 cm^{-1} ; 1468 cm^{-1} . Then, the ammonium salt decomposes above 500°C. The end of decomposition of the montmorillonite modifier is definitively completed at approx. 750°C, *i.e.* much higher than it would seem based directly on the DTG curve analysis (Fig. 5). Above these temperatures, the spectrum of the inorganic part of C15A clay there's only visible.

Figure 7 summarizes the FT-IR spectra made for unheated samples, respectively: PET fibers, PET fibers with the addition of 0.5 wt % C15A, the differential spectrum (DC) obtained by subtracting both of the above-mentioned spectra and the spectrum of pure C15A clay.

Spectroscopic studies of PET fibers without a modifier and after the addition of C15A indicate significant differences in the measurement beam interference with vibrations of oscillators involved in intermolecular interactions. These oscillators include mainly polar moieties that enter into intermolecular interactions, including hydrogen and van der Waals interactions.

The differential spectrum, marked as DS, obtained by subtracting the PET spectrum from the spectrum for PET + 0.5 wt % of C15A clay, reveals the shift in the resonant frequency of the C=O oscillator in the PET ester group at 1740 cm^{-1} . In the spectrum obtained for PET with the addition of C15A clay, it shifts towards higher frequencies which may indicate cleavage of some of the intermolecular bonds. The shift of the subtracted spectrum band towards higher energies is observed as a negative deviation of the subtraction result from the base mean on the part of higher wave numbers with a simultaneous positive deviation of the result of subtraction on the part of lower wave numbers. Similar effects of the subtraction are observed for other areas of subtracted spectra. This can be explained by the strong intercalation of organophilized montmorillonite C15A with the participation of PET macromolecules. We can also observe a shift towards higher resonance frequencies in the case of C–O–C oscillators in the wave numbers range of approx. 1050–1250 cm^{-1} .

Aliphatic chains derived from the C15A clay ammonium salt also interact significantly with aliphatic frag-

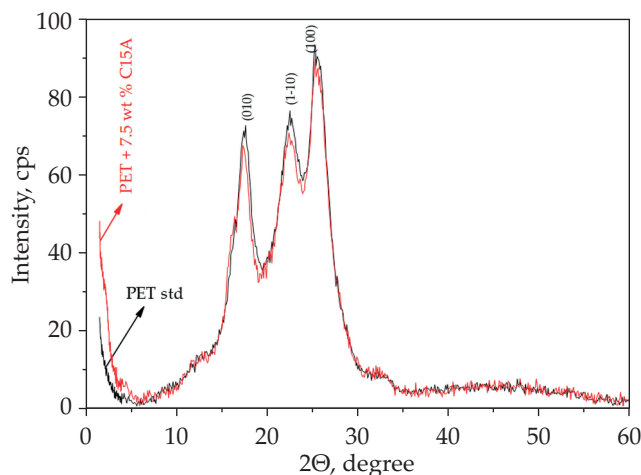


Fig. 8. Examples of WAXS patterns of fibers studied

ments of the PET chain, which is observed in the form of C–H band shifts in the range of approx. 2950 cm^{-1} towards lower wave numbers.

Summing up the above considerations, it can be stated that the results of the FT-IR studies clearly confirm the occurrence of interactions between PET macromolecules and the C15A modifier in the entire temperature range including the oxidative degradation process of the material of the examined fibers – from ambient temperature up to the material ignition. However, in our case, the analysis of recorded spectra does not allow to formulate a categorical conclusion, analogous to that of Liu *et al.* in [35] with respect to nano- $\text{Mg}(\text{OH})_2$, that the addition of nanoclay promotes the formation of condensed carbon structures hindering the migration of decomposition gases into the flame zone, and consequently delaying the ignition itself and slowing down the propagation of the flame zone. Hence, we sought to clarify the essence of the mechanism of combustion inhibition for C15A-modified PET fibers based on X-ray structural studies discussed later in the article.

Nanostructure of studied fibers

In order to determine the effect of C15A nanoclay and its application conditions on the supermolecular structure of PET fibers with flame retardant modification, X-ray studies were carried out, both in the wide (WAXS) and small (SAXS) scattering angles. The tests were carried out for untreated PET fibers, processed only in a water bath at 130°C and for two variants of flame retardant modification – 0.5 wt % (optimal) and 7.5 wt % (maximum tested) content of C15A nanoclay in the bath.

Using the WAXS method, the basic parameters of the fiber crystal structure were determined, including: mass crystallinity degree and average size of crystallites, and the trend of their changes under the influence of the flammable properties modifier was assessed.

Figure 8 shows an example comparison of WAXS curves for PET std and PET + 7.5 wt % C15A fibers. For MMT treated fibers, a slight decrease in the intensity of

Table 1. Crystallinity and dimensions of crystallites obtained by means of WAXS method

| Sample of fibers | Crystallinity κ_{WAXS} , % | Dimensions of crystallites, nm | | |
|-------------------------------|--|--------------------------------|--------------|-------------|
| | | $D_{(010)}$ | $D_{(1-10)}$ | $D_{(100)}$ |
| PET std | 47.0 | 5.9 | 4.6 | 3.7 |
| PET treated in water of 130°C | 49.2 | 5.5 | 4.2 | 3.7 |
| PET + 0.5 wt % C15A | 45.0 | 6.3 | 4.3 | 4.0 |
| PET + 7.5 wt % C15A | 43.9 | 6.4 | 4.5 | 3.7 |

PET crystal peaks can be observed, indicating a slight decrease in the crystallinity of these fibers.

To quantitatively examine the crystallinity of the fibers studied each WAXS curve was deconvoluted into crystalline and amorphous scattering components using the profile fitting program WaxsFit [36].

To evaluate the variations of crystallite sizes of PET, the Scherrer equation [37] was used. The crystallite sizes were calculated in the direction perpendicular to the (010), (1-10) and (100) planes, *i.e.* perpendicular to the PET molecular chain axis. Results are presented in Table 1.

Analysis of the results presented in Table 1 indicates that the treatment of fibers in a water bath without the addition of C15A, during 1 h at 130°C, causes more than 2% increase in the degree of crystallinity. This was to be expected since during high-temperature processing (coinciding with the so-called cold PET crystallization range) the mobility of polymer chains increases to such a degree that further ordering of its structure becomes possible. It should be noted, however, that the addition of C15A in an amount of only 0.5 wt % (optimal modification variant) caused a decrease in the degree of crystallinity by more than 4%. Increasing the amount of nanoclay in the bath to 7.5 wt % caused a further decrease in the degree of fiber crystallinity, but it was disproportionate to the amount of modifier used. The determined values of the average size of crystallites do not show a specific change tendency.

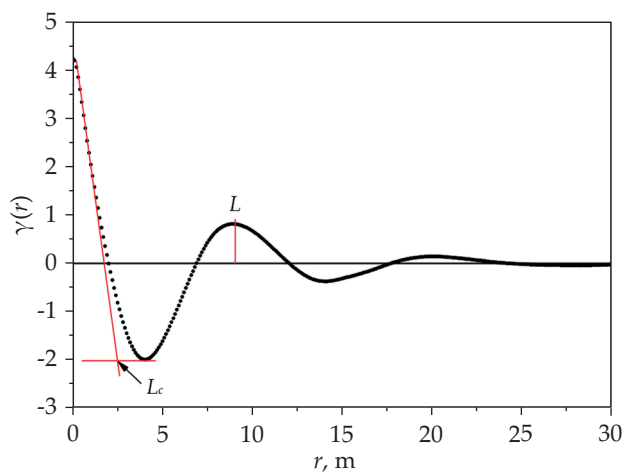


Fig. 9. Correlation function for PET + 0.5 wt % C15A fibers; the figure shows the method of determining the long period (L) and the thickness of the crystal lamellae (L_c)

Table 2. Long period and thicknesses of lamellar structure layers obtained by means of SAXS method

| Sample of fibers | Long period L , nm | Thickness of lamellar structure layers | |
|-------------------------------|----------------------|--|------------|
| | | L_c , nm | L_a , nm |
| PET std | 9.5 | 3.0 | 6.5 |
| PET treated in water of 130°C | 9.4 | 2.9 | 6.5 |
| PET + 7.5 wt % C15A | 9.3 | 2.8 | 6.5 |

Detailed characterization of the lamellar structure of PET fibers was performed by means of the one-dimensional correlation function which was derived from SAXS curves by Fourier transformation. This function allows for determination of the values of the lamellar thickness (L_c) and the amorphous layer thickness (L_a) as well as the long period $L = L_c + L_a$. Figure 9 shows a typical example of the correlation function obtained for one of the samples tested, and shows a method of determining the parameters of a lamellar structure. Results are presented in Table 2.

Analysing the results presented in Table 2, it can be stated that our flame retardant treatment of PET fibers in a water bath used for 1 h at 130°C, both without the addition of a modifier, as well as in the wide range of C15A nanoclay content, causes only minimal fluctuations in parameters of lamellar stacks, which constitute the basic structural element in the commonly assumed and repeatedly verified, fibrillar model of PET fiber structure.

Summing up the structural thread, it should, therefore, be stated that the influence of the modification on the crystal structure of the PET fiber material is very limited. The small, though not negligible, changes in the degree of crystallinity demonstrated by WAXS studies are probably the result of the relatively high processing temperature, and not the effect of C15A nanoclay used as a flame retardant. The crystalline structure of fibers is not fully formed and stabilized due to the conditions of its formation during the spinning process. It is highly mobile to transformation, especially under the influence of relatively long term heating. In our case, it was a 1-hour treatment at temperatures within PET cold crystallization range. Under such conditions, in the absence of more pronounced quantitative changes of crystallinity degree, it is difficult to come to a more categorical conclusion concerning the influence of C15A modifier on the crystalline structure of the fibers.

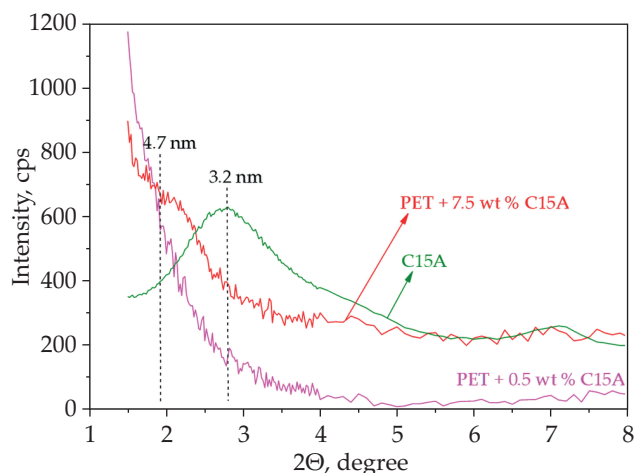


Fig. 10. Comparison of the beginning of WAXS curves taken in the angular range corresponding to the characteristic MMT peak

Flame inhibition mechanism in the use of C15A nanoclay

The inspiration to undertake research in this area was the finding, based on SEM observations, of the existence of a specific coating on the surface of scale formed in the vicinity of the flame (Fig. 4). Since this coating was not observed on the scale after burning of non-modified fibers, it was concluded that its occurrence could be directly related to the flame retardant aluminosilicate used. It is known from literature reports that for the first time an analogous phenomenon was described by K. Yano *et al.* [38] for MMT-containing polyimide nanocomposites. These observations were then confirmed by many authors studying the effect of flame retardation after the introduction of modified montmorillonite nanopowder into various polymer matrices: (polyamide 6) PA6, (polypropylene) PP, (polypropylene/maleic anhydride) PP/MA [39–41], (polystyrene) PS [42]. In all described cases, however, these were typical composite systems made by dispersing aluminosilicate in the matrix polymer melt. In our case, C15A clay dispersed in a water bath was introduced into the material (matrix) of PET fibers not through physical mixing in the melt, but through penetration of the fiber structure from the outside and filling of the so-called “voids” under increased pressure and temperature (130°C) for about 1 hour. Therefore, the question had to be answered: is it possible to create a specific nanocomposite structure with reduced gas permeability in the completely different application conditions that we use?

Research in this area began with the assessment of the degree of dispersion of the aluminosilicate modifier in fibers using the WAXS method.

Figure 10 shows the beginning of the diffraction curves for MMT treated fibers and pure C15A (green), covering the angular range corresponding to the characteristic MMT peak. The interlayer spacing of C15A is 3.2 nm before compounding. In PET + 7.5 wt % C15A (red) the interlayer spacing of MMT increases to 4.7 nm, indicating

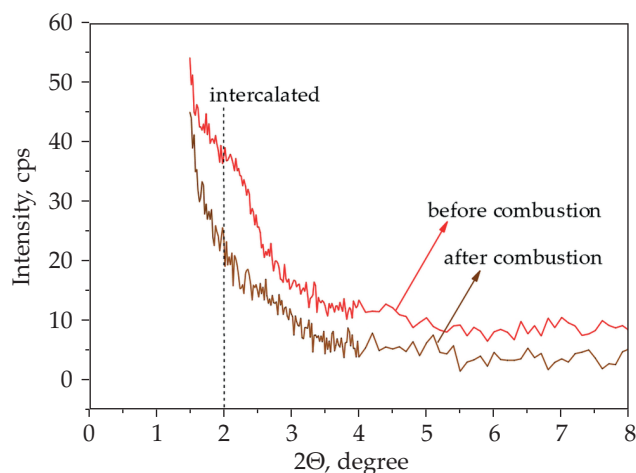


Fig. 11. Comparison of diffraction curves, in the range covering the intercalated C15A peak, for a PET + 7.5 wt % C15A sample before and after combustion

the intercalation of layers, associated with the interaction of MMT with PET chains.

The WAXS curve recorded for fibers with 0.5 wt % C15A content, that is optimal from the point of view of flame retardant properties (pink), in the analyzed angle range is completely smooth. There are no local maxima or even an inflection point, whose location would determine the MMT interlayer distance. In our opinion, the reasons for such a diffraction pattern should not be associated with the occurrence of the modifier exfoliation, but only with too low C15A concentration in the fiber (from the point of view of the WAXS resolution level). The mere demonstration of its intercalation is already extremely important, as it confirms that by using high temperature treatment under increased pressure, it became possible to introduce a modifier of flammable properties into the PET fiber in the solid phase, creating a nanocomposite structure. Based on the above conclusion, an experiment was planned and carried out consisting in fire testing of the modified PET + 7.5 wt % C15A fibers, in which the intercalation of MMT silicate layers was found, and then studying the obtained scale using WAXS method. The curves obtained as a result of the study are presented in Fig. 11.

It turned out that the intercalation effect completely disappears and the curve recorded for the material of fibers subjected to the fire test (black) in the analyzed angle range is completely smooth. There could be only one explanation – the intercalated C15A clay was completely delaminated in the scale. Therefore, the conditions occurred for the exfoliated silicate layers to form a maze-like system that hinders the migration of degradation gas molecules from the depth of the polymer matrix into the flame zone as described in the work of S. Ray and M. Okamoto [43]. In our case, therefore, the distribution of nanoclay in fibers does not play an important role. What is important is the exfoliation of C15A silicate layers in the PET melt, which gradually turns into scale as the temperature increases. The demonstrated effect explains

the flame inhibition mechanism of the flame-retardant modification of PET fibers described by us in the article to a satisfactory degree.

CONCLUSIONS

In the light of the above discussion, it should be acknowledged that the main goals set by us in the course of the research described in the article have been met.

The effectiveness of the flame retardant modification used was demonstrated and its optimal variant (LOI, TGA) was determined. Finally, using the WAXS and SAXS methods, the basic parameters of the nanostructure of the studied fibers were determined, and their nanocomposite nature, expressed by intercalating the layers of C15A nanoclay introduced into the fibers by the PET matrix macromolecules, was confirmed.

The most important goal, on which the research described in the article was primarily focused, was to attempt to explain the mechanism of flame inhibition by the modified C15A aluminosilicate used. SEM microscopy studies demonstrated the formation of a specific coating on the surface of the scale in the immediate vicinity of the flame. Based on previous literature reports, it was assumed that the coating covering the scale effectively hinders the migration of gaseous products into the flame zone, preventing its propagation. Based on the results of diffraction tests, we were able to clearly show the complete delamination of C15A layers in the scale. This allows us to accept the explanation that the consequent system of dispersed silicate plates of the exfoliated C15A modifier is an essential and extremely effective "sealing element" limiting the gas permeability of the system and preventing the spread of flame.

REFERENCES

- [1] Mochane M.J., Luyt A.S.: *Journal of Materials Science* **2015**, 50, 3485.
<http://dx.doi.org/10.1007/s10853-015-8909-0>
- [2] Nazare S., Kandola B.K., Horrocks A.R.: *Polymers Advanced Technologies* **2006**, 17, 294.
<http://dx.doi.org/10.1002/pat.687>
- [3] Entezam M., Khonakdar H.A., Jafari S.M.A. *et al.*: *Journal of Vinyl and Additive Technology* **2017**, 23, E92.
<http://dx.doi.org/10.1002/vnl.21566>
- [4] Ribeiro S.P.S., Martins R.C., Estevão L.R.M. *et al.*: *Microscopy Research and Technique* **2020**, 83, 276.
<http://dx.doi.org/10.1002/jemt.23411>
- [5] Ribeiro S.P.S., Estevão L.R.M., Nova'k C. *et al.*: *Journal of Thermal Analysis and Calorimetry* **2011**, 106, 535.
<http://dx.doi.org/10.1007/s10973-011-1540-7>
- [6] Salaün F., Lemort G., Butstraen C. *et al.*: *Polymers Advanced Technologies* **2017**, 28, 1919.
<http://dx.doi.org/10.1002/pat.4081>
- [7] Ray S.S., Okamoto M.: *Progress in Polymer Science* **2003**, 28, 1539.
<http://dx.doi.org/10.1016/j.progpolymsci.2003.08.002>
- [8] Paul D.R., Robeson L.M.: *Polymer* **2008**, 49, 3187.
<http://dx.doi.org/10.1016/j.polymer.2008.04.017>
- [9] Jancar J., Douglas J.F., Starr F.W. *et al.*: *Polymer* **2010**, 51, 3321.
<http://dx.doi.org/10.1016/j.polymer.2010.04.074>
- [10] Beyer G.: *Plastics, Additives and Compounding* **2002**, 10, 2.
- [11] Horrocks A.R.: *Polymer Degradation and Stability* **2011**, 96, 377.
<http://dx.doi.org/10.1016/j.polymdegradstab.2010.03.036>
- [12] Teli M.D., Kale R.D.: *Polymer Engineering and Science* **2012**, 52, 1148.
<http://dx.doi.org/10.1002/pen.22179>
- [13] Didane N., Giraud S., Devaux E. *et al.*: *Polymer Degradation and Stability* **2012**, 97, 2545.
<http://dx.doi.org/10.1016/j.polymdegradstab.2012.07.006>
- [14] Yang S.-C., Kim J.P.: *Journal of Applied Polymer Science* **2008**, 108, 2297.
<http://dx.doi.org/10.1002/app.27646>
- [15] Carosio F., Laufer G., Alongi J. *et al.*: *Polymer Degradation and Stability* **2011**, 96, 745.
<http://dx.doi.org/10.1016/j.polymdegradstab.2011.02.019>
- [16] Carosio F., Di Blasio A., Cuttica F. *et al.*: *Industrial & Engineering Chemistry Research* **2013**, 52 (28), 9544.
<http://dx.doi.org/10.1021/ie4011244>
- [17] Alongi J., Ciobanu M., Tata J. *et al.*: *Journal of Applied Polymer Science* **2011**, 119, 1961.
<http://dx.doi.org/10.1002/app.32954>
- [18] Kim Y.-H., Jang J., Song K.-G. *et al.*: *Journal of Applied Polymer Science* **2001**, 81, 793.
<http://dx.doi.org/10.1002/app.1497>
- [19] Chen D.-Q., Wang Y.-Z., Hu X.-P. *et al.*: *Polymer Degradation and Stability* **2005**, 88, 349.
<http://dx.doi.org/10.1016/j.polymdegradstab.2004.11.010>
- [20] Guo D.-M., Fu T., Ruan C. *et al.*: *Polymer* **2015**, 77, 21.
<http://dx.doi.org/10.1016/j.polymer.2015.09.016>
- [21] Eckel D.F., Balogh M.P., Fasulo P.D. *et al.*: *Journal of Applied Polymer Science* **2004**, 93, 1110.
<http://dx.doi.org/10.1002/app.20566>
- [22] Gashti M.P., Moradian S.: *Journal of Applied Polymer Science* **2012**, 125, 4109.
<http://dx.doi.org/10.1002/app.35493>
- [23] Gurmendi U., Eguiazabal J.I., Nazabal J.: *Macromolecular Materials and Engineering* **2007**, 292, 169.
<http://dx.doi.org/10.1002/mame.200600376>
- [24] Ghasemi H., Carreau P.J., Kamal M.R. *et al.*: *Polymer Engineering and Science* **2012**, 52, 420.
<http://dx.doi.org/10.1002/pen.22099>
- [25] Rault F., Campagne Ch., Rochery M. *et al.*: *Journal of Polymer Science: Part B: Polymer Physics* **2010**, 48, 1185.
<http://dx.doi.org/10.1002/polb.22008>
- [26] Chuang C.S., Tsai K.C., Yang T.H. *et al.*: *Applied Clay Science* **2011**, 53, 709.

- <http://dx.doi.org/10.1016/j.clay.2011.06.009>
- [27] Devaux E., Rochery M., Bourbigot S.: *Fire and Materials* **2002**, 26, 149.
<http://dx.doi.org/10.1002/fam.792>
- [28] Shahidi S., Ghoranneviss M.: *Journal of Fusion Energy* **2014**, 33, 88.
<http://dx.doi.org/10.1007/s10894-013-9645-6>
- [29] Toda T., Yoshida H., Fukunishi K.: *Polymer* **1997**, 38, 5463.
[http://dx.doi.org/10.1016/S0032-3861\(97\)00093-1](http://dx.doi.org/10.1016/S0032-3861(97)00093-1)
- [30] Fabia J., Gawłowski A., Graczyk T. et al.: *Polimery* **2014**, 59, 557.
<http://dx.doi.org/10.14314/polimery.2014.557>
- [31] *Pat. Appl.* P. 429 004 (2019).
- [32] Gawłowski A., Fabia J., Graczyk T. et al.: *Journal of Thermal Analysis and Calorimetry* **2016**, 125 (3), 1327.
<http://dx.doi.org/10.1007/s10973-016-5498-3>
- [33] Mokhtar N.M., Lau W.J., Ismail A.F. et al.: *RSC Advances* **2014**, 4, 63367.
<http://dx.doi.org/10.1039/C4RA10289D>
- [34] Gawłowski A., Fabia J., Ślusarczyk Cz. et al.: *Polimery* **2017**, 62, 848.
<http://dx.doi.org/10.14314/polimery.2017.848>
- [35] Liu H., Wang R., Xu X.: *Polymer Degradation and Stability* **2010**, 95, 1466.
<http://dx.doi.org/10.1016/j.polyimdegrad-stab.2010.06.023>
- [36] Rabiej M.: *Journal of Applied Crystallography* **2017**, 50, 221.
<http://dx.doi.org/10.1107/S160057671601983X>
- [37] Alexander L.E.: "X-ray Diffraction Methods in Polymer Science", Wiley, New York, USA, 1969.
- [38] Yano K., Usuki A., Okada A. et al.: *Journal of Polymer Science Part A: Polymer Chemistry* **1993**, 31, 2493.
<http://dx.doi.org/10.1002/pola.1993.080311009>
- [39] Gilman J.W.: *Applied Clay Science* **2000**, 15, 31.
[http://dx.doi.org/10.1016/S0169-1317\(99\)00019-8](http://dx.doi.org/10.1016/S0169-1317(99)00019-8)
- [40] Bourbigot S., Bras M.L., Dabrowski F. et al.: *Fire and Materials* **2000**, 24, 201.
[http://dx.doi.org/10.1002/1099-1018\(200007/08\)24:4<201::AID-FAM739>3.0.CO;2-D](http://dx.doi.org/10.1002/1099-1018(200007/08)24:4<201::AID-FAM739>3.0.CO;2-D)
- [41] Gilman J.W., Jackson C.L., Morgan A.B. et al.: *Chemistry of Materials* **2000**, 12, 1866.
<http://dx.doi.org/10.1021/cm0001760>
- [42] Zhu J., Morgan A.B., Lamelas F.J. et al.: *Chemistry of Materials* **2001**, 13, 3774.
<http://dx.doi.org/10.1021/cm000984r>

Received 16 III 2020.